UNIVERSITYOF BIRMINGHAM

Chemical characteristics and source apportionment of particulate matter (PM$_{2.5}$) in Dammam, Saudi Arabia

Alwadei, Manna; Srivastava, Deepchandra; Alam, Mohammed S.; Shi, Zongbo; Bloss, William J.

[Link to publication on Research at Birmingham portal](#)

Chemical characteristics and source apportionment of particulate matter (PM$_{2.5}$) in Dammam, Saudi Arabia: Impact of dust storms

Manna Alwadei [a,*], Deepchandra Srivastava [b], Mohammed S. Alam [c], Zongbo Shi [b], William J. Bloss [b]

[a] Department of Environmental Health, College of Public Health, Imam Abdulrahman Bin Faisal University, Dammam, Saudi Arabia
[b] School of Geography, Earth and Environmental Sciences, University of Birmingham, Edgbaston, Birmingham, B15 2TT, United Kingdom
[c] Division of Agriculture and Environmental Sciences, School of Biosciences, University of Nottingham, Leicestershire, LE12 5RD, United Kingdom

ARTICLE INFO

ABSTRACT

Atmospheric particulate matter (PM) is known to be harmful to human and environmental health, with factors including particle size and composition thought to be key drivers of toxicity. Understanding the composition and hence sources of PM is critical to distinguish between anthropogenic and natural impacts, and develop the most efficient air pollution mitigation policies. This distinction is particularly important in areas affected by dust storm activity from nearby arid regions, which may dominate long-term PM mass concentrations. In this work, 24-hour PM$_{2.5}$ samples were collected from two locations in Dammam city, Saudi Arabia during the winter and summer of 2018, and subjected to detailed analysis to assess the PM characteristics and sources. Offline chemical analysis of the samples utilied ICP/MS, ion chromatography and thermal decomposition for measurement of trace metals, ions and OC/EC concentrations, respectively. Positive Matrix Factorization (PMF) analyses were used to identify sources of PM$_{2.5}$ in Dammam. The mean PM$_{2.5}$ mass concentration in the summer was twice that in the winter at both locations, and crustal and secondary inorganic aerosol components dominated over other species in determining PM$_{2.5}$ mass concentrations at both seasons and locations. The PMF analysis identified six source factors, including crustal, nitrate-rich, sea salt, sulfate-rich, biomass burning and traffic sources. In addition, the impact of dust storms on PM$_{2.5}$ concentrations was analysed. Dust storms increased the 24-hour average concentration of PM$_{2.5}$ by three-fold, and that of crustal elements by five-fold while the impact of dust storms on components identified as anthropogenic in origin was limited. Overall, dust-storm activity accounted for 42% of PM$_{2.5}$ mass concentration; after accounting for this aspect, secondary inorganic components derived largely from primary pollutant emissions dominated the remaining PM$_{2.5}$ mass.

1. Introduction

Acute and chronic exposure to fine particles has been linked with several human health impacts, including cardiovascular diseases, respiratory disorders, mortality and morbidity (Rai et al., 2016; Shi et al., 2019; Hama et al., 2020). The World Health Organization (WHO) has estimated that over than 91% of the 2016 global population was exposed to air pollution levels that exceeded WHO guidelines, and that outdoor ambient air pollution was estimated to cause more than four million premature death each year (WHO, 2018). Understanding the characteristics and sources of airborne particulate matter (PM) is essential to mitigate its impacts on public health, climate, agriculture and economic development.

PM mass concentration is not the only factor determining impacts on human health. Ambient particulate matter with a diameter of less than 2.5 μm (PM$_{2.5}$) typically comprises a mixture of chemical components originating from multiple sources (Geng et al., 2017). The size, shape and chemical composition of PM are thought to be the primary factors in human toxicity, with smaller particles being more toxic than the same mass of large particles, all other factors being equal (Crilley et al., 2017). Moreover, it has been suggested that low-toxicity outcomes are derived from soil dust, sodium chloride and ammonium nitrate, although they make up most of the continental boundary layer of PM$_{2.5}$ mass concentration (Borm et al., 2007; Kundu and Stone, 2014). In contrast,

transition metals that make up a small portion of the total PM$_{2.5}$ mass concentration are thought to cause high-toxicity outcomes (Sørensen et al., 2003; Borm et al., 2007; Kundu and Stone, 2014). Therefore, knowing PM composition in detail can help to assess toxicity, and enable policies to target emission sources associated with the most toxic components, to most effectively reduce health impacts from poor air quality.

PM$_{2.5}$ composition may include organic and elemental carbon, metals and ions, and it may combine both primary species emitted directly to the atmosphere and secondary species formed in it (Contini et al., 2010; Hama et al., 2020). The chemical composition of PM in any area is related to its sources, and to subsequent atmospheric processing-evaporation/condensation, and chemical reactions. These processes affect different components to different extents, depending upon the nature of the particles and the post-emission atmospheric environment. Carbonaceous particles are present in the PM in a considerable fraction, representing 21–78% of PM$_{2.5}$ mass, and they have critical environmental and public health impacts including affecting cardiovascular mortality and morbidity (Pio et al., 2011; Grivas et al., 2012). Metals are emitted into the atmosphere from natural (volcanic activities and soil dust) and anthropogenic sources (fossil fuel composition, vehicle emission and industrial activities), although their relative importance varies substantially with the species considered. Metals are typically stable within the atmosphere following emission, and they may accumulate in the human body, damaging internal organs even at low concentration in the case of elements such as Pb, Cd, As and Cr (Lee et al., 2007; Park and Dam, 2010; González et al., 2017).

In general, sources of PM are considered to be natural or anthropogenic. These two sources may be subdivided into many components, including soil and sea salt as natural while industrial emissions, biomass burning and oil combustion as anthropogenic sources. Distinguishing between these sources from ambient measurements/samples is challenging, especially in the urban environment. Some particles are clearly emitted from natural sources, such as volcanic dust and soil dust, and other particles are clearly emitted from human-made sources, such as industrial and vehicle emission. Nevertheless, some particle components (e.g., biomass burning) can be emitted from natural (forest fire) and anthropogenic (burning wood for cooking and heating) sources where differentiating between natural or anthropogenic sources is difficult, as the overall aerosol particle phase may be both internally and externally mixed. Several methods may be used to evaluate the contribution of various sources to PM. One such method is the enrichment factor (EF) established by Taylor (1964), which can differentiate between the potential natural or anthropogenic sources of PM composition by comparing the ratio of the concentration of an element in the air sample with a reference element (like Al or Fe) that is believed to be entirely from (typically) a crustal source. By using this method, it is possible to compare the relative concentration of a measured element with typical crustal background values (Duan et al., 2006; Haritash and Kaushik, 2007; Murillo-tovar, 2011; Chen et al., 2015). Another approach to distinguish between different PM sources is the receptor-model-based source apportionment (Sharma and Mandal, 2017). Source apportionment uses measurements of PM chemical composition as critical factors to differentiate between sources (Pant and Harrison, 2012). The positive matrix factorisation (PMF) implementation from the United States Environmental Protection Agency (USEPA) (US-EPA, 2014) is an established model for estimating the contribution of each source to PM.

The air quality in Saudi Arabia (SA) is negatively impacted by the prevailing incidence of dust storms and anthropogenic sources from petroleum industries, construction and a rapidly increasing number of vehicles (Farahat, 2016; Lihavainen et al., 2017). Due to the hot weather, arid lands and episodic dust storms, the average PM concentration in SA is higher in hot months than in cold months (Alharbi et al., 2015; Munir et al., 2017). In Makkah, that is located in the west part of SA, the average mass concentration of PM$_{2.5}$ in the summer of 2014 was 88.3 µg/m^3 while it was 67.6 µg/m^3 in the winter of 2015 (Nayebare et al., 2018), in Riyadh, the capital city of SA and is located in the middle

of the country, the PM$_{2.5}$ average mass concentration was 104 µg/m^3 and 76.3 µg/m^3 in the summer and winter of 2006, respectively (Rushdi et al., 2013), and in Hada al Sham (rural area) the average mass concentration of PM$_{2.5}$ was 37 µg/m^3 in the summer and 30 µg/m^3 in the winter (Lihavainen et al., 2016). The most abundant components of PM$_{2.5}$ mass in SA are crustal elements, followed by secondary inorganic ions (NH$_4^+$and SO$_4^-$) (Alharbi et al., 2015; Nayebare et al., 2016; Bian, 2018). Nayebare et al. (2016) studied the source of PM$_{2.5}$ in Rabigh, SA. 24-hour PM$_{2.5}$ samples were collected on PTFE filters using a low volume air sampler in a residential area from 6th May to June 17, 2013. Samples were analysed for mass concentration, black carbon, water-soluble ions and trace elements. The contribution of different sources to PM$_{2.5}$ in Rabigh was predicted using the PMF model. The authors reported five possible sources of PM$_{2.5}$, identified as crustal, heavy oil combustion, industrial dust, vehicle emissions and sea spray. In Jeddah, Khodeir et al. (2012) investigated the composition and sources of PM$_{2.5}$ by collecting 24-hour samples on Teflon filters at seven sites from June to September 2011. Filters were analysed for trace elements using dispersive energy X-ray fluorescence. Five factors were identified for trace PM$_{2.5}$ elements in Jeddah, including crustal, oil combustion, traffic, industrial mix-1 (welding, fine sanding and other metal cutting activities) and industrial mix-2 (polishing and air plastic burning). The crustal factors represented 40% and 51% of the PM$_{2.5}$ sources found in previous studies. Both studies collected samples in hot months only which may be the reason of the high contribution of crustal elements. Moreover, oil combustion, industrial, and traffic factors were all identified as PM$_{2.5}$ components in both studies. However, sea salt was not identified in Jeddah, although it is a coastal city. The industrial mix-2 factor in Jeddah was rich in Cl and Na with Ca, but the absence of Mg led the authors to conclude that this was not from a sea salt source.

Dammam is an urban city located on the east coast of SA. The Arabian Gulf surrounds it to the east and Ad Dahna desert to the west. Dammam is home to more than three million people and is characterised by rapid urbanisation and growth in vehicular traffic. The weather in Dammam is hot, with high humidity throughout the entire year. Usually, temperatures reach 50 °C in the summer, but the temperature range during the winter goes from 0 °C to 25 °C. Cars are the only means of transportation, and the city has different industrial and commercial activities. This study is the first to investigate PM$_{2.5}$ composition and sources in Dammam.

2. Materials and methods

2.1. Sampling

Daily (24-hour period) PM$_{2.5}$ samples were collected at two locations in Dammam, SA, over two periods of two months each, January/ February and July/August 2018. The first location was on the roof (about 15 m above ground level) of the Amanah building, which is in the city centre of Dammam, characterized by a high level of traffic and commercial activities. The second location was on the roof (about 15 m above ground level) of the Public Health college building inside the campus of Imam Abdulrahman bin Faisal University. These locations are referred to as the "City Centre" and "University" locations throughout this work. The PM$_{2.5}$ samples were collected in parallel on pre-baked 100% pure quartz filters and pre-weighed Teflon filters with a 47 mm diameter at each location using MiniVol samplers. Two samplers were utilised at the City Centre location, and two samplers were utilised at the University location simultaneously in both campaigns. A total of 39 daily samples were collected on each of Teflon and Quartz filters for each location and each sampling seasons.

Field blanks were collected prior to, in the middle of and at the conclusion of each sampling period and locations. Filters were stored in petri dishes and frozen directly after collection and shipped frozen to Birmingham for laboratory analysis.

2.2. Laboratory analyses

2.2.1. Organic carbon (OC) and elemental carbon analysis (EC)

The total organic carbon loading, separated into organic (OC) and elemental (EC) carbon fractions was determined by analysing samples collected on the quartz filters for the amount of carbon evolved as a function of temperature. Organic and elemental carbon were measured using a DRI Model 2015 Multiwavelength Thermal/Optical Carbon Analyzer using the EUSAAR2 protocol (Crilley et al., 2015; Vodička et al., 2015). Before the samples were analysed, lab blank calibration was performed daily. Device control calibration using sucrose was performed every second to confirm performance stability; all sucrose results were constant. All results were corrected using field blank filters, which resulting in a subtraction of 0.5 µg/cm^2 for OC and 0 µg/cm^2 for EC.

2.2.2. Water soluble ions (WSI)

Each quartz filter was extracted in 5 ml of 18.2 MΩ-cm deionised water using 15 ml centrifuge tubes. Extraction solutions were refrigerated until the time of analysis. All field blank filters were extracted and treated like samples. Water soluble ions were analysed via a Dionex ICS 1100 ion chromatograph fitted with the IONPAC AS22 2 × 250 mm column to measure anions, while Dionex™ Integrion HPIC fitted with (Dionex™ ionpac cg12a) column for cations. For quality control, a certified reference material (CRM) was used for cation and anion standards. Additional details are described elsewhere (Song et al., 2020). All results were corrected using field blank filter results, and correction ranged from 2% to 20% of total measured WSI.

2.2.3. Metal analysis

PM$_{2.5}$ was extracted from samples collected on quartz filters by adding 10 ml of 68% ultrapure nitric acid using microwave digestion vessels. Vessels were placed in a Mars-6 Microwave Digestion System (CEM). The digestion acid samples were diluted with 2% HNO$_3$ concentration (16.6-fold dilution) required for using inductively coupled plasma mass spectrometry (ICP-MS).

Metals were measured using ICP-MS. For quality control and testing of the repeatability of the instruments, a standard reference material (Media-NIST, particulate on filter) was analysed with each set of extractions (Loyola et al., 2009; González et al., 2017). Extraction efficiency was high (more than 80%) for most elements, except for Al and Ti. All results were corrected using field blank filter results which ranged from 0% (no target compounds were detected) to 10% of the measured metal concentrations.

2.3. Data approaches

2.3.1. Source apportionment

PM sources in Dammam were quantified by the EPA implementation of positive matrix factorization (PMF) analysis (version 5.0.14). PMF is a model that uses mathematical approaches to estimate the contribution of different sources based on their unique fingerprint (US-EPA, 2014). Many researchers have used PMF to determine the sources of PM. A data matrix X of i (number of samples) by j (chemical species) is calculated in the presence of uncertainty (u). PMF solves the mass balance between source profiles and species concentrations through the number of p factors, based on equation (2):

$$X_{ij} = \sum_{k=1}^{p} g_{ik} f_{jk} + e_{ij} \qquad (2)$$

where (X) is the matrix of the number of samples (i) each composed of the number of chemical species (j), (p) is the number of factors and the mass concentration (g) of each species contributing to each sample (i) multiplied by each factor (k). (e_{ij}) is the residual for each species. The uncertainty in the concentration of each species for PMF inbut was calculated using equation (3):

$$Unc = \sqrt{(Error\ Fraction\ \times concentration)^2 + (0.5\ \times MDL)^2} \qquad (3)$$

MDL is the method detection limit. The error fraction was calculated by dividing the standard deviation of the concentration obtained for the measured reference material, treated as samples, by the average of these measured material concentrations. PMF does not accept zero or negative input values. The concentration of species which were below the MDL was replaced by half of the MDL, while the uncertainty assigned to species whose concentration was below the MDL was calculated using equation (4):

$$Unc = \frac{5}{6}\ \times MDL \qquad (4)$$

There are no specific criteria for choosing the number of factors in PMF. In this case, the model was initially instructed to run four factors initially. Then, the number of factors was increased step-wise until nine factors were included. Several criteria were applied to choose the best sources solution, including the difference between Q (Robust) and Q (True), the value of Q $_{(True)}$/Q $_{(expected)}$ needs to be 1 or close to 1 and the coefficient of variation between the predict and measured PM$_{2.5}$ elements.

3. Results and discussion

3.1. PM$_{2.5}$ mass concentration

In Table 1, the mean and standard deviation of the concentrations of PM$_{2.5}$, metals, water-soluble ions, OC and EC within PM$_{2.5}$ are shown for the City Centre and University sites for the winter and summer

Table 1

Mean concentrations and standard deviation of PM$_{2.5}$, metals, water-soluble ions, OC and EC at City Centre and University sites during the winter and summer 2018 campaigns.

Species	Winter		Summer	
	City Centre	University	City Centre	University
	Mean ± SD	Mean ± SD	Mean ± SD	Mean ± SD
PM$_{2.5}$ (µg/m^3)	63.9 ± 49.1	54.2 ± 31.6	121.2 ± 66.9	114.7 ± 65.6
Metals (ng/m^3)				
Al	2420 ± 2358.7	2229.7 ± 2656.8	3399.3 ± 3687.6	3909.9 ± 4383.8
Ti	76.6 ± 92.9	71.3 ± 107.0	178.6 ± 209.3	189.7 ± 209.6
Mn	25.6 ± 26.6	19.5 ± 22.0	52.1 ± 48.3	56.7 ± 51.6
Fe	1053.8 ± 1381.5	955 ± 1353.0	2512.6 ± 2536.4	2818.5 ± 2768.4
Co	0.7 ± 0.7	0.6 ± 0.7	1.6 ± 1.6	1.7 ± 1.6
Cu	372.3 ± 373	220.5 ± 193.4	81.5 ± 95.7	63.3 ± 75.1
Ni	17 ± 21.5	19.5 ± 21.6	36.4 ± 23.4	26.9 ± 17.7
V	8 ± 4.0	7.7 ± 4.2	14.5 ± 8.2	18.1 ± 8.3
As	0.6 ± 0.5	0.7 ± 0.4	0.9 ± 0.7	0.7 ± 0.7
Sr	14.6 ± 14.5	13.1 ± 17.5	30.4 ± 28.8	34.6 ± 30.9
Sn	27.3 ± 1 4.9	31.1 ± 26.4	99.5 ± 49.2	117.7 ± 39.4
Sb	5.5 ± 6.8	3 ± 4.5	2.9 ± 3.1	2 ± 1.6
Ba	20.9 ± 20.6	37.7 ± 78.5	30.1 ± 23.9	82.9 ± 79.9
Pb	30.8 ± 45.4	26.7 ± 35.3	36.5 ± 48.0	36.2 ± 70.4
WSI (µg/m^3)				
Na$^+$	0.4 ± 0.2	0.4 ± 0.2	0.6 ± 0.4	0.9 ± 0.5
NH$_4^+$	3.9 ± 3.0	4.1 ± 3.8	4.4 ± 2.2	5 ± 2.2
K$^+$	0.17 ± 0.1	0.1 ± 0.1	0.2 ± 0.1	0.2 ± 0.2
Mg^{2+}	0.16 ± 0.16	0.2 ± 0.2	0.3 ± 0.2	0.5 ± 0.3
Ca^{2+}	1.6 ± 2.4	1.9 ± 3.2	4.5 ± 3.9	6.2 ± 5.2
Cl$^-$	0.54 ± 0.2	0.6 ± 0.5	0.8 ± 0.5	0.8 ± 0.5
SO$_4^{2-}$	7 ± 3.5	87 ± 5.0	13.2 ± 4.9	15.6 ± 6.5
NO$_3^-$	3.4 ± 2.1	3.9 ± 2.5	2.7 ± 1.4	2.8 ± 1.2
OC and EC (µg/m^3)				
OC	6.3 ± 3.0	6.2 ± 2.9	7.8 ± 3.9	8 ± 4.2
EC	1.8 ± 0.8	2 ± 0.7	1.9 ± 1.4	2 ± 1.4

measurement campaigns during 2018.

The mean mass concentration of $PM_{2.5}$ was similar at the two locations for both the winter and summer campaigns. The time-series of $PM_{2.5}$ mass concentration at the two locations tracked each other closely (Fig. S1), indicating a regional pattern of $PM_{2.5}$ abundance, and that any local sources, specific to just one of the sampling locations, has a small impact on $PM_{2.5}$ concentrations. In winter, the daily $PM_{2.5}$ mass concentration was above the World Health Organisation (WHO) guideline for maximum 24 h (25 $\mu g/m^3$) (WHO, 2021), except for three and four days during the 39-day-campaign at City Centre and University, respectively. $PM_{2.5}$ concentrations at both locations were above the WHO guideline for the maximum $PM_{2.5}$ concentration per 24-h for all samples collected in the summer.

The mean $PM_{2.5}$ concentration in Dammam in summer (118 $\mu g/m^3$) was a factor of 1.9 higher than that observed in the winter (60 $\mu g/m^3$). This is similar to previous results. For example, $PM_{2.5}$ concentrations in the summer were 1.4 times higher than that in the winter in Riyadh and Makkah (Rushdi et al., 2013; Nayebare et al., 2018), and 1.2 times higher in the summer than in the winter in Huda Al-Sham, a rural area about 60 km to the east of Jeddah ((21.802° North, 39.729° East) (Lihavainen et al., 2016). This was attributed to dry weather that leads to dust storms and facilitate lofting of particles from the ground to the atmosphere (Farahat, 2016).

3.2. Organic carbon and elemental carbon (OC and EC)

Both OC and EC concentrations were similar at the City Centre and University sites (Table 1). Mean OC concentrations were significantly higher in the summer than in the winter at both locations ($P < 0.05$). The mean EC concentrations showed no significant seasonal variation, similarly to the observations of Grivas et al. (2012). It is apparent from Fig. 1 that OC and EC concentrations at both locations tracked each other, suggesting a similar background loading from regional sources (such as industry) rather than local sources specific to either site (such as local road traffic).

3.2.1. OC/EC ratio

EC is emitted directly as a primary pollutant from the incomplete combustion of carbonaceous matter, whereas OC can be emitted directly (primary OC) or formed in it the atmosphere (Pio et al., 2011; Grivas et al., 2012; Zhao et al., 2013). The OC/EC ratio may be used as a tracer to evaluate the sources of carbonaceous matter in the atmosphere (Pio et al., 2011). An OC/EC ratio in sources aerosols below or around 1.0 is indicative of samples impacted by diesel emission or oil combustion sources, and higher OC/EC ratios (e.g. ≥ 3.4) are associated with gasoline combustion emission sources (Chow et al., 2011; Pio et al., 2011;

Fig. 1. The OC and EC time series in the $PM_{2.5}$ mass for City Centre (blue and orange lines) and University (grey and yellow lines) sites during the summer and winter sampling 2018 seasons. (For interpretation of the references to colour in this figure legend, the reader is referred to the Web version of this article.)

Grivas et al., 2012). The presence of secondary organic aerosols contributes to a higher OC/EC ratio. The OC/EC ratio was higher during the summer than during the winter at both locations. There was no significant difference between the City Centre and University locations in the two seasons, suggesting similar sources at both locations.

In the winter, the OC/EC mean ratio was 3.9 and 3.2 for the City Centre and University sites, respectively. In the summer the mean OC/EC mean ratio was 4.8 at the City Centre and 5.2 at the University location. In both locations and seasons OC/EC ratios were above 3.0 (Fig. S4). Such values indicate the impact of gasoline, which is the primary fuel used in Saudi Arabian cars and accounts for 69% of transportation fuel consumed (Howarth et al., 2020).

3.3. Water soluble ions (WSI)

During the winter, the most abundant WSI measured was SO_4^{2-} followed by NH_4^+ and NO_3^- at both locations. However, during the summer, Ca^{2+} was the second most abundant ionic species after SO_4^{2-}. The Ca^{2+} had a higher mean concentration than NH_4^+ and NO_3^- potentially because of the influence of crustal-derived components during the summer from dust storms. The mean total WSI mass analysed during the winter was 17.2 $\mu g/m^3$ at City Centre and 20 $\mu g/m^3$ at the University. In comparison, the mean total measured ion concentrations during the summer were 26.8 $\mu g/m^3$ and 32.2 $\mu g/m^3$ at City Centre and University, respectively. Even though the mean total measured WSI concentration was higher during the summer than during the winter, the contribution of the WSI to the total $PM_{2.5}$ mass was higher during the winter at both locations. The total ion contribution to the $PM_{2.5}$ mass during the winter was 33.2% and 41% at City Centre and University, respectively. During the summer, the total ion contribution was 25.8% at the City Centre and 33.2% at the University location (Fig. S2). The lower contribution of total ions during the summer compared to the winter is due to the high $PM_{2.5}$ concentration caused by a higher incidence of dust storms during summer, as shown by the high concentration of crustal elements (Table 1).

SO_4^{2-}, NH_4^+ and NO_3^- were the most abundant WSI species, representing more than 80% of the total measured WSI during the winter and more than 75% during the summer at both locations. The high contribution of these three secondary inorganic species is similar to results reported elsewhere (Masiol et al., 2015; Sharma and Mandal, 2017; Xiao et al., 2020; Yang et al., 2020). SO_4^{2-}, NH_4^+ and NO_3^- are secondary inorganic species which are mainly formed in the atmosphere from gas-to-particle transformation (Xiao et al., 2020; Yang et al., 2020; Su et al., 2021).

3.4. Crustal and trace elements

Overall, there was no significant difference between the mean metal concentrations at the City Centre and University locations in either of the two seasons (Table 1). On average, crustal elements, such as Al, Fe and Ti, were more abundant than other elements, as expected in arid areas. These three elements represented more than 88% and 94% of the total measured metal mass concentrations during the winter and summer, respectively. This shows a substantial impact of crustal elements on the $PM_{2.5}$ mass in Dammam. Concentrations of all other metals analysed were below 100 ng/m^3, except for Cu at both locations in the winter (Table 1). Both Co and As had mean concentration below 1 ng/m^3 at both locations during the winter. During the summer, all non-crustal metals had a mean concentration below 100 ng/m^3, except for Sn at the University location. The seasonal variation for trace elements indicates a strong dust impact on PM mass concentration in the summer. Nonetheless, Cu and Sb, which are sometimes considered as non-exhaust road traffic particles (Loyola et al., 2009; Park and Dam, 2010; González et al., 2017), reached higher concentrations during the winter than in the summer ($P < 0.05$). The traffic volume is lower during the summer when it is the vacation period.
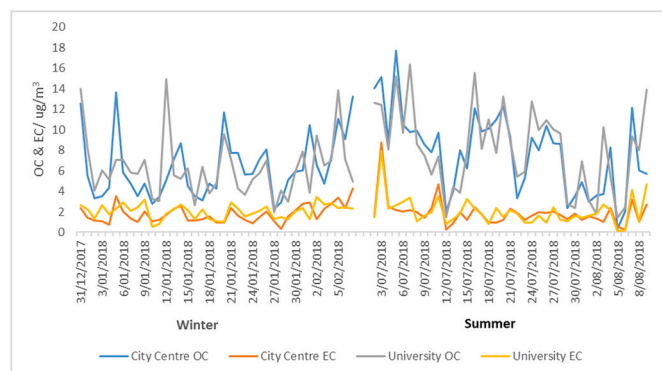
The mean measured total mass of metals in PM$_{2.5}$ was higher during the summer than during the winter. During the winter, the mean total mass of metals was 4 μg/m^3 and 3.6 μg/m^3 at the City Centre and the University sites. During the summer, the mean total mass of metals was 6.5 μg/m^3 at the City Centre and 7.4 μg/m^3 at the University site. However, the opposite pattern was observed for the contribution of metals (combined) to the total PM$_{2.5}$ mass, where the total metal contribution during the winter was higher than that observed during the summer. The mean contributions of metal species to the total PM$_{2.5}$ mass was 6.3% and 6.7% at the City Centre and the University sites during the winter, respectively. During the summer, the mean total metal contribution at the City Centre was 5.3% and 6.4% at the University location, as shown in (Fig. S3).

3.5. Mass closure

The mass closure for PM$_{2.5}$ in Dammam was evaluated as the sum of the mass concentrations of the oxides of Al (Al$_2$O$_3$), Fe (Fe$_2$O$_3$), Mn (MnO), Ti (TiO$_2$), Ca (CaCo$_3$) and OM (OM = OC x 1.6 (Squizzato et al., 2016; Masiol et al., 2020)) in addition to concentrations of other measured species, including other ions measured in this work (Mg^{2+}, Na$^+$, K$^+$ and Cl$^-$) and other metals measured in this work (Co, Cu, Ni, V, As, Sr, Sn, Sb, Ba and Pb). It was not possible to quantify the mass

concentration of Si (hence SiO$_2$), so Si was estimated from Al mass concentration assuming Si = Al x 3.83 (Perrone et al., 2016). Thus, the "crustal" crustal category presented here is the sum of Al$_2$O$_3$, Fe$_2$O$_3$, MnO, TiO$_2$, CaCO$_3$ and estimated SiO$_2$. The unexplained mass (termed "others" in Fig. 2), which are unmeasured species or aerosol bound water, was calculated as the different between gravimetrically determined total PM$_{2.5}$ mass and the sum of measured components (estimated in the case of (SiO$_2$) mass. In the winter, the crustal components represented 38% and 40% of the average PM$_{2.5}$ mass concentration in the City Centre and University locations, respectively (Fig. 2). Secondary inorganic aerosols (ammonium, sulfate and nitrate) represented 22% and 30% of the average PM$_{2.5}$ mass in the City Centre and University, respectively. Organic matter contributed to 16% and 18% followed by elemental carbon (3% and 4%), other ions (2% and 3%), and other metals (1% and 1%) at each location. Non-measured components (others) represented 18% and 4% of PM$_{2.5}$ at the City Centre and the University, respectively (Fig. 2). In the summer, the contribution of crustal components increased from 38% at the City Centre site to 52%, and from 40% at the University to 50%, indicating the impact of greater occurrence of dust storms. Secondary inorganic aerosols were the second largest component (after crustal) of the average mass closure of PM$_{2.5}$ contributing to 17% and 20% in the City Centre and University, respectively. The organic matter contribution to the average mass

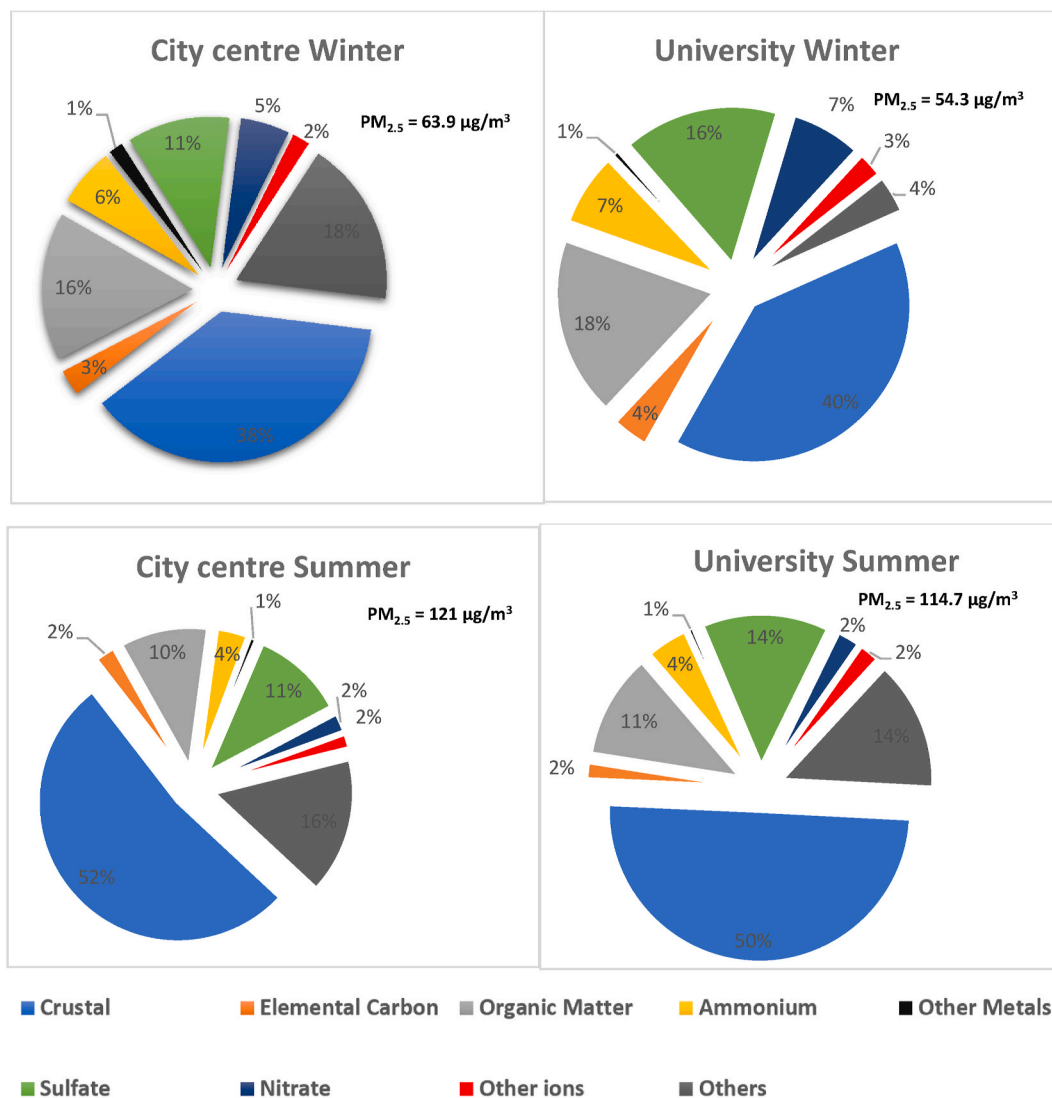**Fig. 2.** Major chemical components of PM$_{2.5}$ in Dammam collected in the winter and summer of 2018 where "Crustal" is the sum of Al$_2$O$_3$, Fe$_2$O$_3$, MnO, TiO$_2$, CaCo$_3$ and estimated SiO$_2$, "Other Ions" is the sum of Mg^{2+}, Na$^+$, K$^+$ and Cl$^-$, "Other Metals" is the sum of Co, Cu, Ni, V, As, Sr, Sn, Sb, Ba and Pb.

closure decreased in the summer from 16% to 10% at the City Centre site, and from 18% to 11% at the University site. Elemental carbon contributions reduced from 3% to 4% in the winter to 2% in the summer in both locations. The contribution of other ions was 2% at both locations, and other metals were responsible for 1% of $PM_{2.5}$ mass concentration at both sites (considering their elemental masses only, not oxides). The unexplained mass in the summer was 16% at the City Centre and 14% at the University location (Fig. 2).

3.6. Source apportionment using PMF

PMF analysis was undertaken on the entire dataset, combining all sample analysis results for both locations and seasons. A six-factor solution was identified to provide the best source solution for this study, as it had the minimum difference between Q (Robust) and Q (True) and the closet Q (True)/Q expected value (1.4) of the optimal solution value (1.0). Moreover, the six-factor solution has the highest coefficient of variation between the predicted and measured $PM_{2.5}$ ($r^2 = 0.859$), and provides physically realistic interpretation of the sources of aerosol particles at the locations. The factor source profiles for the six-factor solution are shown in Fig. 3. In the following sections, we discuss the characteristics and identities of each factor/source.

3.6.1. Factor one (nitrate-rich factor)

This factor was dominated by NO_3^- (71.9% of which was in this factor), EC (39.2% of which was in this factor), OC (27.2% of which was in this factor) (Fig. 3). These components are likely to be mainly of secondary origin. Nitrate is a secondary particle component formed in the atmosphere from the oxidation of NO_x, which in turn is emitted from many sources, such as traffic, ships, biomass burning and agricultural activities (Tan et al., 2017; Dadashazar et al., 2019). Power plants and traffic emissions may be key sources of this factor because they are responsible for more than 55% and 25% of the NO_x emission in SA (Europrean Commision, 2018). This factor may contain contributions from shipping activities in the Arabian Gulf, as ships added 4%–12% to particulate nitrate in the coastal area (Dai and Wang, 2021). The timeseries of this factor (Fig. S5) showed a same trend for both sites, indicating regional rather than local sources, and the level of this factor was higher in the winter than that in the summer, consistent with lower temperature favouring the formation of NO_3^- (Kim and Hopke, 2012). This factor contributed to 12% of the $PM_{2.5}$ in Dammam.

3.6.2. Factor two (sea salt

This factor was characterized by high contribution of Mg^{2+} (80.9% of which was in this factor), Na^+ (58% of which was in this factor), Ca^{2+}

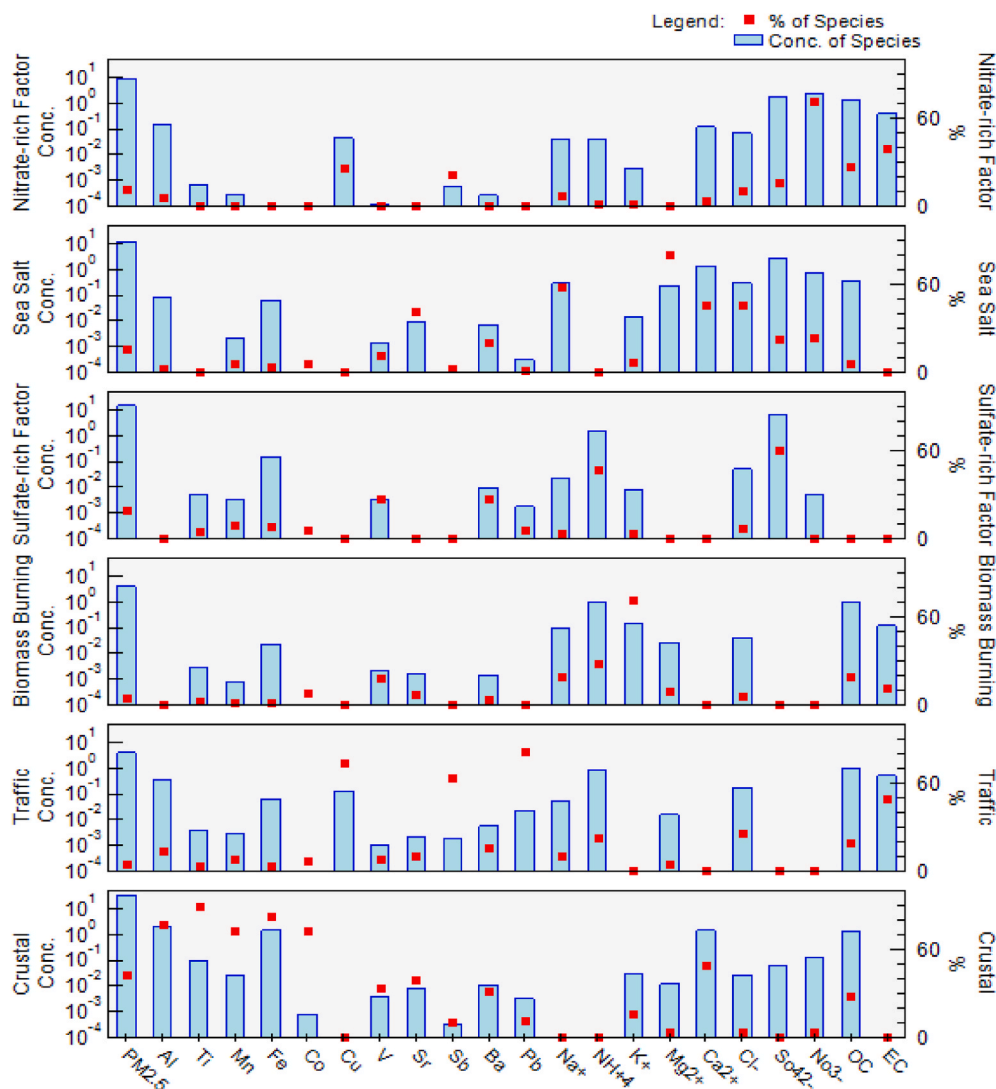**Fig. 3.** Factor profiles for the factors identified with the PMF analysis. Blue bars refer to the concentration (µg/m³, left hand axis), whereas red squares refer to the percentage contribution of each species (right hand axis). (For interpretation of the references to colour in this figure legend, the reader is referred to the Web version of this article.)

(46.5% of which was in this factor), Cl$^-$ (45.6% of which was in this factor), which are typically sea salt. The "sea salt" factor was estimated by PMF to contribute to 15.6% of PM$_{2.5}$ in Dammam.

3.6.3. Factor three (sulfate-rich factor)

The third factor contributing to the PM$_{2.5}$ in Dammam was rich with sulfate and ammonium. This factor was dominated mostly by SO$_4{}^{2-}$ (60% of which was in this factor), NH$_4{}^+$ (47% of which was in this factor) and V (27% of which was in this factor), as can be seen in Fig. 3. Sulfate and ammonium are mainly formed in the atmosphere from SO$_2$ and NH$_3$ (Liu et al., 2014b; Tan et al., 2017). The element V is commonly linked to oil combustion, including a potential contribution from shipping oil combustion (Cesari et al., 2014; Dadashazar et al., 2019). The main sources of SO$_2$ are likely power plants and industrial activities (Kim et al., 2004; Tsai et al., 2013; Nayebare et al., 2016; Rai et al., 2016) and shipping emissions (Cesari et al., 2014, 2016; Dadashazar et al., 2019). Oil combustion is the primary fuel used in SA to generate electricity. The sources of SO$_2$ in Dammam were investigated using Community Emissions Data System (CEDS) (McDuffie et al., 2020). The results of this inventory showed that 53% of SO$_2$ was from industry and 44% was from energy generation. Thus, these two sources are responsible for about 97% of SO$_2$ emission in Dammam. Also, Dammam is located on the Arabian Gulf, which receives many ships exporting oil from SA to the world, and others bringing goods from around the globe to SA and other Arabian Gulf countries and Iran. This factor was responsible for 19% of the PM$_{2.5}$ in Dammam.

3.6.4. Factor four (biomass burning)

This factor was characterised by a high contribution of K$^+$ (71.4% of which was in this factor), NH$_4{}^+$ (28.1% of which was in this factor), OC (18.8% of which was in this factor) and EC (11.6% of which was in this factor) (Fig. 3). This factor is likely linked to biomass burning due to the high abundances of K$^+$ and OC (Cesari et al., 2014, 2016; Dadashazar et al., 2019). There could be two main sources for this factor. The first is agricultural activities on date palms plantations located some 15 km to the northwest of Dammam. Stubble is burned off after harvest and before planting crops to improve the agricultural land and to kill the Red Palm Weevil and palms infected by it, protecting others. This possibility was inspected by pollution rose analysis using the open-air package in R (Carslaw, 2015), as shown in Fig. 4. More than 30% of this factor was explained by the farm area, with wind direction indicating impact upon both sampling locations. The second source could be related to waste incinerators, as suggested by (Kim et al., 2004; Lomozik et al., 2004; Cheng et al., 2015). Waste incinerators exist in different areas around Dammam, mainly in the northwest and southwest areas of the city.

According to the PMF analysis, this factor was estimated to be the source of 5.2% of the PM$_{2.5}$ in Dammam. The contribution of this source, while not negligible, is low compared to that found in other studies worldwide, which have found this source to be typically 9%–24% of PM mass (Kundu and Stone, 2014; Rai et al., 2016; Dadashazar et al., 2019; Liu et al., 2020).

3.6.5. Factor five (traffic factor)

This factor was characterised by a high contribution of Pb (81.7% of which was in this factor), Cu (74.2% of which was in this factor), Sb (63.5% of which was in this factor), EC (49.1% of which was in this factor), Cl$^-$ (26.2% of which was in this factor) and OC (19.3% of which was in this factor), as can be seen in Fig. 3. These elements are typically markers for traffic emissions. EC is considered a typical marker for vehicle exhaust emission, while elements like Cu, Mn, Zn and Pb are associated with vehicle wear particles (such as brakes or tyres) (Thorpe and Harrison, 2008; Pant and Harrison, 2012; Crilley et al., 2017; Srivastava et al., 2018). The timeseries of this factor (Fig. S6) illustrated some variation between the two locations, suggesting the impact of local sources (vehicle emission). This factor was estimated by the PMF analysis to be the source of 5% of PM$_{2.5}$ in Dammam.

3.6.6. Factor six (crustal factor)

This factor was characterised by a high contribution of Al (77% of which was associated with this factor), Ti (88.9% of which was associated with this factor), Mn (72.6% of which was associated with this factor), Fe (82.7% of which was associated with this factor) and Ca^{2+} (49.4% of which was associated with this factor), as can be seen in Fig. 3. These elements are typically crustal (Lomozik et al., 2004; Liu et al., 2014; Crilley et al., 2017). Construction and cement work, widely seen during the sampling campaigns in the surroundings, may have contributed to this factor (Bernardoni et al., 2011; Crilley et al., 2017). The timeseries of this factor (Fig. S7) was similar to the timeseries of PM$_{2.5}$ mass concentration (Fig. S1) demonstrating the impact of dust storm activity on this factor. This factor contributed to more than 40% of the PM$_{2.5}$ in Dammam. This is comparable to the contribution reported in earlier studies in similar settings, such as Rabigh (SA) and Tunis (Tunisia) by Nayebare et al. (2016) and Kchih et al. (2015).

3.7. Impact of dust storms on PM$_{2.5}$ composition and sources

The regular occurrence of dust storms is expected in Saudi Arabia. There was one dust storm during the sampling collection in the winter and three dust storms in the summer. Here, winter dust storm periods were defined as any sample with a PM$_{2.5}$ mass concentration of more
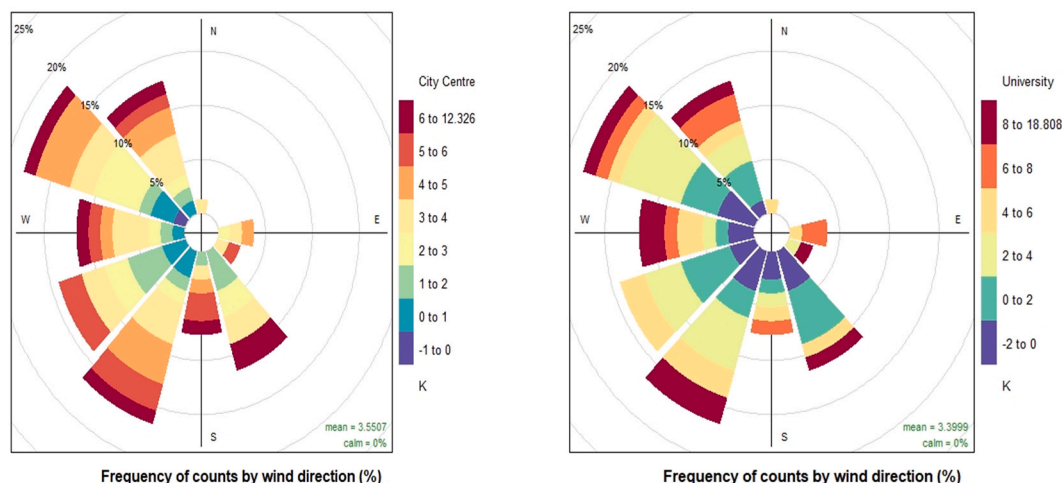

Fig. 4. Pollution rose graph of the biomass burning factor at the City Centre (left) and the University (right).

than 100 μg/m^3 (4 out of 39 samples), and summer dust storm periods were defined as any sample which had a PM$_{2.5}$ mass concentration of more than 150 μg/m^3 (7 out of 39 samples).

The mean PM$_{2.5}$ mass concentration during dust storm days was approximately 3-fold higher than that during the non-dust storm days in both seasons, as shown in Table 2. Interestingly, the mean PM$_{2.5}$ mass concentration of non-dust storm days in the summer (90 μg/m^3) was two times higher than that in the winter (45.4 μg/m^3). Also, the mean mass concentration of PM$_{2.5}$ in the summer (226.3 μg/m^3) during dust storm days was 1.6 times higher than that in the winter (137 μg/m^3). This finding indicates the negative impact of summer-via increased dust storm activity-on the PM concentration in SA. The crustal metal (Al, Fe, Ti and Mn) concentrations were five times higher during dust period samples than non-dust samples, and the contribution of these elements to PM$_{2.5}$ mass was 2-fold higher during dust storms compared to non-dust storms (Fig. S8). There is little difference in trace element concentrations, with or without dust storms (Fig. S9). Concentration of the crustal ion Ca^{2+} also increased by approximately 3-fold during dust storms during the winter and summer. Also, the mean OC concentrations during the dust storms were significantly higher than the overall mean values in both winter and summer (Table 2) similar to results reported elsewhere (Liu et al., 2014a; Lovett et al., 2018). Yet, dust storms had a limited impact on the concentration of EC or water-soluble ions, apart from calcium and magnesium.

The PMF analysis was rerun using data from non-dust-storm-influenced samples only to show the contribution of each PM$_{2.5}$ factor without the impact of dust storms. The contribution of the crustal factors reduced from 43.2% to 23.7%, the sulfate-rich factor increased from 18.9% to 25.8%, the nitrate-rich factor increased from 12% to 20.2%, the sea salt factor increased from 15.6% to 19%, the biomass burning factor increased from 5.2% to 6% and the traffic factor increased from 5% to 5.3%, as shown in Fig. 5.

Table 2

The mean PM$_{2.5}$ concentration and its composition in samples of non-dust-storms and dust storm days.

Species	Winter		Summer	
	Non-dust samples	Dust samples	Non-dust samples	Dust samples
PM$_{2.5}$ (μg/m^3)	45.4	**137 ****	90	**226.3 ****
Metals (ng/m^3)				
Al	1548.1	**6791.7****	1960.4	**10343.9****
Ti	42.3	**247.3 ****	106.2	**488.6 ****
Mn	16.5	**61.2 ****	34.5	**132.4 ****
Fe	592.6	**3516.2 ****	1553.9	**7019.1 ****
Co	0.4	**1.7 ****	1	**4.2 ****
Cu	**305.2**	243.5	**76.5**	58
Ni	**19.8**	12.6	24.9	**51.5 ****
V	6.9	**14 ****	13.5	**27 ****
As	**0.7**	0.5	0.6	**1.5 ****
Sr	10.4	**28.7 ****	22	**72.7 ****
Sn	**31.8 ****	5.5	**120 ****	74.9
Sb	4.2	**6.2**	2.1	**3.4**
Ba	27.4	**35.7**	51.2	**73.4**
Pb	25.9	**40.9**	**37**	31.2
WSI (μg/m^3)				
Na$^+$	0.3	**0.5 ***	0.7	**1.2 ****
NH^{+4}	**4.2**	2.7	**5.1 ****	3
K$^+$	0.15	**0.2**	0.2	**0.3 ****
Mg^{2+}	0.13	**0.4 ****	0.4	**0.7 ****
Ca^{2+}	1	**6.2 ****	3.6	**12 ****
Cl$^-$	0.5	**0.7**	0.7	**1.2 ****
SO$_4^{2-}$	7.8	7.8	14.3	**14.6**
NO$_3^-$	3.5	**4.2**	2.5	**3.6 ****
OC and EC (μg/m^3)				
OC	6.00	**7.7 ***	7.1	**11.1 ****
EC	**1.89**	1.85	**1.71**	1.17

(Higher values are in **bold**). (* significantly at p < 0.05). (** significantly at p < 0.01).

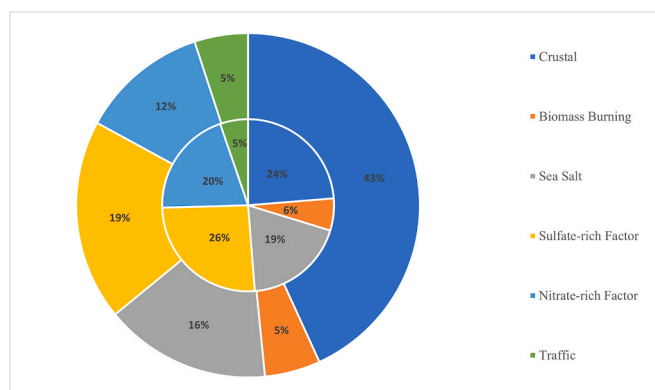**Fig. 5.** Relative contribution of different factors to PM$_{2.5}$ mass during non-dust days (inner circle) compared to all days (outer circle).

Removing dust storm episodes leaves the sulfate-rich factor as the most significant contributor to PM$_{2.5}$ in Dammam (rather than being placed second, after the crustal factor, as was found using all samples, including dust storm periods). Additionally, in non-dust samples, crustal elements contributed to less than a quarter of the PM mass compared to about half of PM mass when dust storms were included. Dust storms had little impact on biomass and traffic factors where biomass burning and traffic contribution was 5.2% and 5% for all samples and 6% and 5.2% for non-dust samples respectively, suggesting that the contribution of these factors to PM$_{2.5}$ mass in Dammam is modest.

4. Conclusions

We report measurements of PM$_{2.5}$ mass concentration, composition and sources in Dammam, Saudi Arabia. The level of PM$_{2.5}$ was high in Dammam during the winter and summer in the urban/suburban locations explored. Seasonal variations showed a higher PM$_{2.5}$ level during the summer, which was twice that found in the winter. The mean PM$_{2.5}$ concentration in Dammam was 45.4 μg/m^3 in samples from non-dust days and 139 μg/m^3 in samples from dusty days during the winter. During the summer, the mean PM$_{2.5}$ concentration was 90 μg/m^3 for non-dust days and 226.4 μg/m^3 in samples from dusty days. Although relative to many anthropogenic sources, potentially less can be done to mitigate the impact of dust storms on arid areas, especially in countries in the Arabian Gulf, planting trees around and inside cities could potentially reduce resuspended dust as well as increase deposition (Nowak et al., 2014). Despite the impact of dust storms and desert soil, the mean concentrations of anthropogenic elements (SO$_4^{2-}$ and OC) were higher than those of all other elements, including crustal elements.

In the PMF analysis, it was possible to identify six factors as primary sources of PM$_{2.5}$ in Dammam, including crustal, sulfate-rich factor, sea salt, nitrate-rich factor, biomass burning and traffic. Among these factors, crustal and sea salt factors are essentially natural sources, representing about 60%, while other anthropogenic sources represent 40% of PM$_{2.5}$ mass concentrations in Dammam. However, removing dust-storm periods reduces the contribution of natural sources to 42% while secondary inorganic sources together were responsible for about 46% of PM$_{2.5}$ in Dammam. As secondary aerosols are formed in the atmosphere from primary pollutants, controlling primary sources would lead to significant improvements in air quality in Dammam. The contribution of traffic emissions to PM$_{2.5}$ was lower than many results found in other literature studies (Kim et al., 2004; Cheng et al., 2015; Tan et al., 2017), which may be due to the low percentage of diesel vehicles compared to gasoline vehicles in Dammam.

Quantitative assessment of PM$_{2.5}$ sources, explicitly considering the impacts of/allowing for the influence of dust storm data, gives a clearer picture of anthropogenic sources to PM$_{2.5}$ in Dammam, and hence of priorities for clean air policy measures.

CRediT authorship contribution statement

Manna Alwadei: Conceptualization, Methodology, Software, (EPA PMF), Data curation, Writing – original draft, Formal analysis. **Deepchandra Srivastava:** helped with EPA PMF software running. **Mohammed S. Alam:** Methodology, Writing – review & editing. **Zongbo Shi:** Visualization, Investigation, Supervision. **William J. Bloss:** Supervision, Visualization, Investigation, Project administration, Validation, Conceptualization.

Declaration of competing interest

The authors declare that they have no known competing financial interests or personal relationships that could have appeared to influence the work reported in this paper.

Acknowledgement

Appendix A. Supplementary data

Supplementary data to this article can be found online at https://doi.org/10.1016/j.aeaoa.2022.100164.

References

Alharbi, B., Shareef, M.M., Husain, T., 2015. Study of chemical characteristics of particulate matter concentrations in Riyadh, Saudi Arabia. Atmos. Pollut. Res 6 (1), 88–98. https://doi.org/10.5094/APR.2015.011. Elsevier.

Bernardoni, V., et al., 2011. PM10 source apportionment in Milan (Italy) using time-resolved data. Sci. Total Environ. 409 (22), 4788–4795. https://doi.org/10.1016/j.scitotenv.2011.07.048. Elsevier B.V.

Bian, Q., 2018. Supplement of Sources of PM 2 . 5 Carbonaceous Aerosol in Riyadh. Saudi Arabia', pp. 3969–3985.

Borm, P.J.A., et al., 2007. 'Oxidant Generation by Particulate Matter: from Biologically Effective Dose to a Promising, Novel Metric', *Occupational And Environmental Medicine*, pp. 73–74. https://doi.org/10.1136/oem.2006.029090.

Carslaw, D., 2015. The Openair Manual Open-Source Tools for Analysing Air Pollution Data. King's College London, p. 287 (January).

Cesari, D., et al., 2014. Source apportionment of PM2.5 in the harbour-industrial area of Brindisi (Italy): identification and estimation of the contribution of in-port ship emissions. Sci. Total Environ. 497–498, 392–400. https://doi.org/10.1016/j.scitotenv.2014.08.007. Elsevier B.V.

Cesari, D., et al., 2016. Inter-comparison of source apportionment of PM10 using PMF and CMB in three sites nearby an industrial area in central Italy. Atmos. Res. 182, 282–293. https://doi.org/10.1016/j.atmosres.2016.08.003. Elsevier B.V.

Chen, P., et al., 2015. 'Assessment of Heavy Metal Pollution Characteristics and Human Health Risk of Exposure to Ambient PM2.5 in Tianjin, China', *Particuology*, vol. 20. Chinese Society of Particuology, pp. 104–109. https://doi.org/10.1016/j.partic.2014.04.020.

Cheng, Y., et al., 2015. 'PM2.5 and PM10-2.5 Chemical Composition and Source Apportionment Near a Hong Kong Roadway', *Particuology*, vol. 18. Chinese Society of Particuology, pp. 96–104. https://doi.org/10.1016/j.partic.2013.10.003.

Chow, J.C., et al., 2011. PM2.5 source profiles for black and organic carbon emission inventories. Atmos. Environ. https://doi.org/10.1016/j.atmosenv.2011.07.011.

Commision, Eurprean, 2018. EDGAR: the Emissions Database for Global Atmospheric Research Leaflet. EU Open Data portal. Available at: https://edgar.jrc.ec.europa.eu/EDGAR-infographics.pdf. (Accessed 1 July 2021).

Contini, D., et al., 2010. Characterisation and source apportionment of PM10 in an urban background site in Lecce. Atmos. Res. 95 (1), 40–54. https://doi.org/10.1016/j.atmosres.2009.07.010. Elsevier B.V.

Crilley, L.R., et al., 2015. Sources and contributions of wood smoke during winter in London: assessing local and regional influences. Atmos. Chem. Phys. 15 (6), 3149–3171. https://doi.org/10.5194/acp-15-3149-2015.

Crilley, L.R., et al., 2017. Source apportionment of fine and coarse particles at a roadside and urban background site in London during the 2012 summer ClearfLo campaign. Environ. Pollut. 220, 766–778. https://doi.org/10.1016/j.envpol.2016.06.002. Elsevier Ltd.

Dadashazar, H., Ma, L., Sorooshian, A., 2019. Sources of pollution and interrelationships between aerosol and precipitation chemistry at a central California site. Sci. Total Environ. 651, 1776–1787. https://doi.org/10.1016/j.scitotenv.2018.10.086. Elsevier B.V.

Dai, J., Wang, T., 2021. Impact of International Shipping Emissions on Ozone and PM 2 . 5. The Important Role of HONO and ClNO 2', pp. 1–29. February).

Duan, F.K., et al., 2006. Concentration and chemical characteristics of PM2.5 in Beijing, China: 2001-2002. Sci. Total Environ. 355 (1–3), 264–275. https://doi.org/10.1016/j.scitotenv.2005.03.001.

Farahat, A., 2016. Air pollution in the Arabian Peninsula (Saudi Arabia, the United Arab Emirates, Kuwait, Qatar, Bahrain, and Oman): causes, effects, and aerosol categorization. Arabian J. Geosci. 9 (3) https://doi.org/10.1007/s12517-015-2203-y.

Geng, G., et al., 2017. Chemical composition of ambient PM2. 5 over China and relationship to precursor emissions during 2005-2012. Atmos. Chem. Phys. 17 (14), 9187–9203. https://doi.org/10.5194/acp-17-9187-2017.

González, Lucy T., et al., 2017. Determination of Trace Metals in TSP and PM 2 . 5 Materials Collected in the Metropolitan Area of Monterrey , Mexico : A Characterization Study by XPS. Atmos. Res. 8–22. https://doi.org/10.1016/j.atmosres.2017.05.009. Elsevier, 196(May).

González, Lucy T., et al., 2017. Determination of Trace Metals in TSP and PM2.5 Materials Collected in the Metropolitan Area of Monterrey, Mexico: A Characterization Study by XPS, ICP-AES and SEM-EDS. Atmos. Res. 8–22. https://doi.org/10.1016/j.atmosres.2017.05.009. Elsevier, 196(April).

Grivas, G., Cheristanidis, S., Chaloulakou, A., 2012. Elemental and organic carbon in the urban environment of Athens. Seasonal and diurnal variations and estimates of secondary organic carbon. Sci. Total Environ. 414, 535–545. https://doi.org/10.1016/j.scitotenv.2011.10.058. Elsevier B.V.

Hama, S.M.L., et al., 2020. Four-year assessment of ambient particulate matter and trace gases in the Delhi-NCR region of India. Elsevier Sustain. Cities Soc. 54, 102003. https://doi.org/10.1016/j.scs.2019.102003. December 2019.

Haritash, A.K., Kaushik, C.P., 2007. Assessment of seasonal enrichment of heavy metals in respirable suspended particulate matter of a sub-urban Indian City. Environ. Monit. Assess. 128 (1–3), 411–420. https://doi.org/10.1007/s10661-006-9335-1.

Howarth, N., Lanza, A., Shehri, T. Al, 2020. 'Saudi Arabia's 2018 CO2 Emissions Fall Faster than Expected', pp. 1–16. Available at: https://www.kapsarc.org/research/publications/saudi-arabias-2018-co2-emissions-fall-faster-than-expected/. (Accessed 11 June 2021).

Kchih, H., Perrino, C., Cherif, S., 2015. Investigation of desert dust contribution to source apportionment of PM10 and PM2.5 from a southern Mediterranean coast. Aerosol Air Qual. Res. 15 (2), 454–464. https://doi.org/10.4209/aaqr.2014.10.0255.

Khodeir, M., et al., 2012. Source apportionment and elemental composition of PM2.5 and PM10 in Jeddah city, Saudi Arabia. Atmos. Pollut. Res. 3 (3), 331–340. https://doi.org/10.5094/APR.2012.037. Elsevier.

Kim, E., Hopke, P.K., 2012. Source apportionment of fine particles in Washington, DC, utilizing temperature-resolved carbon fractions. Taylor & Francis Group 54 (7), 773–785. https://doi.org/10.1080/10473289.2004.10470948.

Kim, E., et al., 2004. Factor analysis of Seattle fine particles. Aerosol. Sci. Technol. 38 (7), 724–738. https://doi.org/10.1080/02786820490490119.

Kundu, S., Stone, E.A., 2014. Composition and sources of fine particulate matter across urban and rural sites in the Midwestern United States. Environ. Sci. J. Integr. Environ. Res.: Process. Impact. Royal Soc. Chem. 16 (6), 1360–1370. https://doi.org/10.1039/c3em00719g.

Lee, C.S.L., et al., 2007. Heavy metals and Pb isotopic composition of aerosols in urban and suburban areas of Hong Kong and Guangzhou, South China-Evidence of the long-range transport of air contaminants. Atmos. Environ. 41 (2), 432–447. https://doi.org/10.1016/j.atmosenv.2006.07.035.

Lihavainen, H., et al., 2016. Aerosols physical properties at Hada Al Sham, western Saudi Arabia. Atmos. Environ. 135, 109–117. https://doi.org/10.1016/j.atmosenv.2016.04.001.

Lihavainen, H., et al., 2017. Aerosol optical properties at rural background area in Western Saudi Arabia. Atmos. Res. 197 (June), 370–378. https://doi.org/10.1016/j.atmosres.2017.07.019. Elsevier.

Liu, Q., et al., 2014a. Chemical characteristics and source apportionment of PM 10 during Asian dust storm and non-dust storm days in Beijing. Atmos. Environ. 91, 85–94. https://doi.org/10.1016/j.atmosenv.2014.03.057. Elsevier Ltd.

Liu, Q., et al., 2014b. Chemical Characteristics and Source Apportionment of PM10 during Asian Dust Storm and Non-dust Storm Days in Beijing. Atmos. Environ. vol. 91, 85–94. https://doi.org/10.1016/j.atmosenv.2014.03.057. Elsevier Ltd.

Lomozik, M., Szaja, G., Nowak, W., 2004. Source apportionment of fine particles in Washington, dc, utilizing temperature-resolved carbon fractions. J. Air Waste Manag. Assoc. 54 (7), 773–785. https://doi.org/10.1080/10473289.2004.10470948.

Lovett, C., et al., 2018. Oxidative potential of ambient particulate matter in Beirut during Saharan and Arabian dust events. Atmos. Environ. 188, 34–42. https://doi.org/10.1016/j.atmosenv.2018.06.016. Elsevier Ltd.

Loyola, J., et al., 2009. Concentration of airbone trace metals in a bus station with a high heavy-duty diesel fraction', *Journal of the Brazilian Chemical Society*. Sociedade Brasileira de Quimica 20 (7), 1343–1350. https://doi.org/10.1590/S0103-50532009000700020.

Masiol, M., et al., 2015. Spatial, Seasonal Trends and Transboundary Transport of PM2.5 Inorganic Ions in the Veneto Region (Northeastern Italy). Atmos. Environ. vol. 117, 19–31. https://doi.org/10.1016/j.atmosenv.2015.06.044. Elsevier Ltd.

Masiol, M., et al., 2020. Hybrid multiple-site mass closure and source apportionment of PM2.5 and aerosol acidity at major cities in the Po Valley. Sci. Total Environ. 704, 135287. https://doi.org/10.1016/J.SCITOTENV.2019.135287. Elsevier.

McDuffie, E.E., et al., 2020. A global anthropogenic emission inventory of atmospheric pollutants from sector- and fuel-specific sources (1970-2017): an application of the Community Emissions Data System (CEDS). Earth Syst. Sci. Data 12 (4), 3413–3442. https://doi.org/10.5194/essd-12-3413-2020.

Munir, S., et al., 2017. Analysing PM2.5 and its association with PM10 and meteorology in the arid climate of Makkah, Saudi Arabia. Aerosol Air Qual. Res. 17 (2), 453–464. https://doi.org/10.4209/aaqr.2016.03.0117.

Murillo-tovar, M., 2011. Enrichment Factor and Profiles of Elemental Composition of PM 2 . 5 in the City of Guadalajara, pp. 545–549. https://doi.org/10.1007/s00128-011-0369-x. Mexico.

Nayebare, S.R., et al., 2016. Chemical characterization and source apportionment of PM 2.5 in Rabigh, Saudi Arabia. Aerosol Air Qual. Res. 16 (12), 3114–3129. https://doi.org/10.4209/aaqr.2015.11.0658.

Nayebare, S.R., et al., 2018. Ambient Air Quality in the Holy City of Makkah: A Source Apportionment with Elemental Enrichment Factors (EFs) and Factor Analysis (PMF). Environ. Pollut. vol. 243, 1791–1801. https://doi.org/10.1016/j.envpol.2018.09.086. Elsevier Ltd.

Nowak, D.J., et al., 2014. Tree and forest effects on air quality and human health in the United States. Environ. Pollut. 193, 119–129. https://doi.org/10.1016/j.envpol.2014.05.028.

Pant, P., Harrison, R.M., 2012. Critical review of receptor modelling for particulate matter : a case study of India. Atmos. Environ. 49, 1–12. https://doi.org/10.1016/j.atmosenv.2011.11.060. Elsevier Ltd.

Park, K., Dam, H.D., 2010. Characterization of metal aerosols in PM10 from urban, industrial, and asian dust sources kihong Park · hung duy Dam. Environ. Monit. Assess. 160, 289–300. https://doi.org/10.1007/s10661-008-0695-6.

Perrone, M.R., et al., 2016. Saharan dust impact on the chemical composition of PM10 and PM1 samples over south-eastern Italy. Arabian J. Geosci. 9 (2), 1–11. https://doi.org/10.1007/s12517-015-2227-3.

Pio, C., et al., 2011. OC/EC ratio observations in Europe : Re-thinking the approach for apportionment between primary and secondary organic carbon. Atmos. Environ. 45 (34), 6121–6132. https://doi.org/10.1016/j.atmosenv.2011.08.045. Elsevier Ltd.

Rai, P., et al., 2016. Composition and source apportionment of PM1 at urban site Kanpur in India using PMF coupled with CBPF. Atmos. Res. 178–179, 506–520. https://doi.org/10.1016/j.atmosres.2016.04.015. Elsevier B.V.

Rushdi, A.I., et al., 2013. Air quality and elemental enrichment factors of aerosol particulate matter in Riyadh City, Saudi Arabia. Arabian J. Geosci. 6 (2), 585–599. https://doi.org/10.1007/s12517-011-0357-9.

Sharma, S.K., Mandal, T.K., 2017. Chemical composition of fine mode particulate matter (PM2.5) in an urban area of Delhi, India and its source apportionment. Urban Clim. 21, 106–122. https://doi.org/10.1016/j.uclim.2017.05.009. Elsevier B.V.

Shi, Z., et al., 2019. Introduction to the special issue "in-depth study of air pollution sources and processes within Beijing and its surrounding region (APHH-Beijing)". Atmos. Chem. Phys. 19 (11), 7519–7546. https://doi.org/10.5194/acp-19-7519-2019.

Sørensen, M., et al., 2003. Linking exposure to environmental pollutants with biological effects. In: Mutation Research - Reviews in Mutation Research. Elsevier, pp. 255–271. https://doi.org/10.1016/j.mrrev.2003.06.010.

Squizzato, S., et al., 2016. Factors, origin and sources affecting PM1 concentrations and composition at an urban background site. Atmos. Res. 180, 262–273. https://doi.org/10.1016/J.ATMOSRES.2016.06.002. Elsevier.

Srivastava, D., et al., 2018. Speciation of organic fraction does matter for source apportionment. Part 1: a one-year campaign in Grenoble (France). Sci. Total Environ. 624, 1598–1611. https://doi.org/10.1016/j.scitotenv.2017.12.135. Elsevier B.V.

Su, J., et al., 2021. Insights into measurements of water-soluble ions in PM2.5 and their gaseous precursors in Beijing. J. Environ. Sci. (China) 102, 123–137. https://doi.org/10.1016/j.jes.2020.08.031. Elsevier B.V.

Tan, J., et al., 2017. Chemical Characteristics and Source Apportionment of PM2.5 in Lanzhou, China. Sci. Total Environ. vols. 601–602, 1743–1752. https://doi.org/10.1016/j.scitotenv.2017.06.050. Elsevier B.V.

Taylor, S.R., 1964. Abundance of chemical elements in the continental crust: a new table. Geochem. Cosmochim. Acta 28, 1273–1285.

Thorpe, A., Harrison, R.M., 2008. Sources and properties of non-exhaust particulate matter from road traffic : a review. Sci. Total Environ. 400 (1–3), 270–282. https://doi.org/10.1016/j.scitotenv.2008.06.007. The. Elsevier B.V.

Tsai, Y.I., et al., 2013. Source indicators of biomass burning associated with inorganic salts and carboxylates in dry season ambient aerosol in Chiang Mai Basin, Thailand. Atmos. Environ. 78, 93–104. https://doi.org/10.1016/j.atmosenv.2012.09.040. Elsevier Ltd.

US-EPA, 2014. EPA Positive M Atrix Factorization (PM F) 5 . 0 Fundamentals and. Environmental Protection Agency Office of Researc and Development, Publushing House Whashington, DC 20460, p. 136.

Vodička, P., et al., 2015. Detailed comparison of OC/EC aerosol at an urban and a rural Czech background site during summer and winter. Sci. Total Environ. 518 (519), 424–433. https://doi.org/10.1016/j.scitotenv.2015.03.029.

WHO, 2018. Ambient (Outdoor) Air Pollution. Https://Www.Who.Int/En/News-Room/Fact-Sheets/Detail/Ambient-(Outdoor)-Air-Quality-and-Health. Available at: https://www.who.int/news-room/fact-sheets/detail/ambient-(outdoor)-air-quality-and-health. (Accessed 21 July 2021).

WHO (no date), 2021. Air Pollution - Ambient Air Pollution. Available at: https://www.who.int/news-room/fact-sheets/detail/ambient-(outdoor)-air-quality-and-health. (Accessed 2 July 2021). Accessed:

Xiao, H., et al., 2020. Chemical characteristics of major inorganic ions in PM2.5 based on year-long observations in Guiyang, southwest China-Implications for formation pathways and the influences of regional transport. Atmosphere 11 (8). https://doi.org/10.3390/ATMOS11080847.

Xu, J., Song, S., et al., 2020. An interlaboratory comparison of aerosol inorganic ion measurements by ion chromatography: implications for aerosol pH estimate. Atmos. Meas. Tech. 13 (11), 6325–6341. https://doi.org/10.5194/amt-13-6325-2020.

Yang, L., et al., 2020. Characteristics and formation mechanisms of secondary inorganic ions in PM2.5 during winter in a central city of China: based on a high time resolution data. Elsevier Atmos. Res. 233, 104696. https://doi.org/10.1016/j.atmosres.2019.104696. October 2018.

Zhao, P., et al., 2013. Characteristics of Carbonaceous Aerosol in the Region of Beijing, Tianjin, and Hebei, China. Atmos. Environ. 71, 389–398. https://doi.org/10.1016/j.atmosenv.2013.02.010.